Proc. Natl. Acad. Sci. USA
Vol. 87, pp. 6423–6427, August 1990
Biophysics

Molecular characteristics of recombinant human CD4 as deduced from polymorphic crystals

(AIDS/crystallization/immune recognition/molecular shape/signal transduction)

PETER D. KWONG†, SEONG-EON RYU†, WAYNE A. HENDRICKSON†‡§, RICHARD AXEL†‡, ROBERT M. SWEET¶, GAIL FOLENA-WASSERMAN‖, PRESTON HENSLEY‖, AND RAYMOND W. SWEET‖

†Department of Biochemistry and Molecular Biophysics and ‡The Howard Hughes Medical Institute, College of Physicians and Surgeons, Columbia University, New York, NY 10032; ¶Biology Department, Brookhaven National Laboratory, Upton, NY 11973; and ‖SmithKline Beecham Pharmaceuticals, King of Prussia, PA 19406

Contributed by Richard Axel, June 5, 1990

ABSTRACT **We have grown crystals of a soluble recombinant form of human CD4, a transmembrane glycoprotein found predominantly on the surface of helper T cells. Crystals composed of the entire extracellular portion of CD4 exhibit extensive polymorphism. Of the five crystal types that have been grown, the best diffracts to Bragg spacings of 4.9 Å. Symmetry considerations and characterization of the asymmetric unit by volume-specific amino acid analysis lead to the suggestion that a tetramer is the fundamental unit of crystallization. The characterization also showed that several of the crystal types have unusually high solvent contents. Because high solvent content and weak diffraction are indicative of an extended flexible structure, we examined the molecular shape of the recombinant CD4 with ultracentrifugation and found that it has an axial ratio of roughly 6, when modeled as a prolate ellipsoid. These results, combined with crystal packing constraints, suggest dimensions of approximately 25 × 25 × 125 Å for a monomer. The structural features deduced here may be relevant to the biological function of CD4 as a receptor mediating cell–cell and cell–virus interactions.**

The surface glycoprotein CD4 shares sequence and structural properties with immunoglobulins (1). Molecules within this gene family function as recognition proteins; they interact with either soluble ligand or cell surface molecules to mediate cell–cell interactions (2). CD4 mediates the specific association of T helper cells with appropriate antigen-bearing target cells by interacting with major histocompatibility complex class II molecules on the surface of target cells (3–5). In man, CD4 also serves as the receptor for the human immunodeficiency virus by virtue of a high-affinity interaction with gp120, the viral envelope glycoprotein (6–9).

CD4 consists of four extracellular domains, a transmembrane domain, and a cytoplasmic segment. The N-terminal extracellular domain shows sequence homology to immunoglobulin κ light chain variable domains (1). Moreover, epitope mapping with CD4 antibodies suggests that this domain is likely to fold in a manner analogous to variable regions (10, 11). *In vitro* mutagenesis experiments have defined a discrete region within the first domain of CD4 required for high-affinity binding to gp120 (10, 12) but the precise domains required for the association of CD4 with class II molecules have not been defined. The molecular basis for the specific recognition events mediated by CD4 awaits the elucidation of the structure of the CD4 molecule. We describe here five crystal types of a recombinant CD4 molecule that comprises the four extracellular domains of the mature receptor. From analysis of these crystals, we deduce molecular characteristics of shape and association.

The publication costs of this article were defrayed in part by page charge payment. This article must therefore be hereby marked "*advertisement*" in accordance with 18 U.S.C. §1734 solely to indicate this fact.

MATERIALS AND METHODS

Purification of Recombinant Soluble CD4 (sCD4). The extracellular portion of CD4 was expressed in a CHO clone containing a CD4 gene with a termination codon at the extracellular boundary of the transmembrane domain and purified as described (13). The purified protein was concentrated to 4.8 mg/ml by adsorption on an S-Sepharose column (Pharmacia) and dialyzed in 50 mM sodium phosphate (pH 7.0). A portion of this concentrated protein was treated to remove sialic acid with insoluble neuraminidase (Sigma; 0.1 unit of neuraminidase per ml, 0.15 unit of neuraminidase per mg of sCD4) for 12 hr at 37°C in 10 mM EDTA/50 mM sodium acetate, pH 6.0. The desialated protein was dialyzed against 10 mM sodium cacodylate/25 mM ammonium sulfate, pH 6.7, and concentrated to 5.5 mg/ml by centrifugation in a Centricon-10 microconcentrator (Amicon).

Gel Filtration. Purified sCD4 was analyzed by FPLC on a Superose 12 column (Pharmacia). The column was calibrated with blue dextran, bovine serum albumin, ovalbumin, and cytochrome *c* (Sigma). Gel filtration was done at room temperature with a flow rate of 0.4 ml/min in 50 mM sodium phosphate/150 mM NaCl, pH 7.2, or in 50 mM sodium/potassium phosphate/150 mM NaCl, pH 8.8.

Crystallization. Crystals were grown by "hanging-droplet" vapor diffusion (14). Conditions were screened by combining 1 μl of protein solution with 1 μl of crystallization solution (containing diluted precipitant and crystallization additives). The resultant 2-μl droplets were placed over 1.0-ml reservoirs of precipitant and concentrated to a final volume of ≈0.25 μl. Promising conditions were refined with larger droplets (Table 1).

Diffraction Characterization of Crystals. All crystals were mounted directly from hanging droplets without stabilization. X-ray diffraction data were recorded on CEA Reflex-25 film with 1.105-Å or 1.220-Å radiation at station X12-C, National Synchrotron Light Source (NSLS), Brookhaven National Laboratory. Space groups were determined by first aligning crystals with still photographs and then checking for symmetry and systematic absences in 2.0° oscillation photographs. Unit-cell dimensions from crystal types A, D, and E were evaluated through the processing of densitometered films (DENZO program; Z. Otwinowski, Yale University), and direct measurements from principal zones were used for the others. In general, cell parameters were determined at minimum Bragg spacings of 7–10 Å. Systematic absences and symmetry described here may break down at higher resolution. Also, the measurements contain an estimated uncertainty of 0.5% in λ, 0.8% in crystal to film distance, and 1.0%

Abbreviation: sCD4, soluble CD4.

§To whom reprint requests should be addressed at: Department of Biochemistry and Molecular Biophysics, Columbia University, 630 West 168th Street, New York, NY 10032.

in measurement of Bragg spacings on film. These result in a 1.4% uncertainty in the measurement of the cell parameters given in Table 2.

Characterization of Crystal Contents. The number of molecules per asymmetric unit (Z_a) was determined by the following procedure: a crystal was mounted in a glass capillary and its dimensions were optically measured at a magnification of ×100 to find crystal volume; amino acid analysis was carried out to find the number of molecules in the crystal; and, given the unit-cell volume and space-group symmetry, Z_a could then be calculated directly from the resulting number of molecules per crystal volume.

The solvent content was calculated from Z_a, the space group parameters, the molecular weight, and the partial specific volume of the recombinant sCD4 [protein component, 41.03 kDa and 0.7445 cm^3/g (as calculated from the amino acid composition); carbohydrate component, 4.0 kDa and 0.65 cm^3/g (as calculated from two N-linked biantennary carbohydrates with 50% sialic acid addition, ref. 15)].

Amino Acid Analysis. Mounted crystals used to characterize crystal contents were transferred to glass hydrolysis tubes for amino acid analysis. Care was taken to minimize the amount of transferred mounting capillary and mother liquor. Capillary contents were vacuum dried to remove water, hydrolyzed with vapor-phase hydrochloric acid, and applied to an amino acid analyzer (Applied Biosystems, derivatizer–analyzer model 420A). By using a 2-aminohexanoic acid standard to correct for experimental losses and by correlating the amino acid analysis with the known amino acid composition, the number of molecules in the original sCD4 crystal sample was determined.

Survey of Crystallization Data Base. Solvent contents were calculated as described above with parameters (space group, molecular weight, and Z_a) extracted from the crystallization data base [G. L. Gilliland (Center for Advanced Research in Biology), from Protein Data Bank deposit]. For proteins the partial specific volume was assumed to be 0.73 cm^3/g, and for nucleic acids it was assumed to be 0.50 cm^3/g.

Ultracentrifugation. Velocity analytical ultracentrifugation studies of sCD4 were carried out in a Beckman model E ultracentrifuge equipped with a photoelectric scanner and a temperature control system. Double-sector cells with charcoal-filled Epon center pieces and quartz windows were used. The protein concentration was 1.0 mg/ml in 50 mM sodium phosphate/0.15 M NaCl, pH 7.5, 20°C.

RESULTS AND DISCUSSION

Protein Characterization. The purified sCD4 used in these studies migrated as a single band on 0.1% SDS/polyacrylamide gels. Structural analysis by mass spectrometry confirmed a homogeneous amino acid sequence but also detected variable sialic acid and fucose additions at the two asparagine-linked carbohydrate attachment sites (15). By native PAGE at pH 8.8, the sialic acid heterogeneity was reflected by at least five bands, consistent with the mass spectrometry-derived biantennary carbohydrate structure. Treatment of sCD4 with neuraminidase removed most of this charge heterogeneity (Fig. 1).

In the mass spectrometry analysis, ≈50% of the carbohydrate was found to be fucosylated, but less than 10% of the sCD4 used in this study bound to lentil lectin, which recognizes fucosylated biantennary carbohydrates (data not shown). Gel filtration showed the protein to be homogenous with respect to its oligomeric state under dilute conditions. At pH 7.2 and pH 8.8, sCD4 eluted as a monomer at 60.0 kDa and 59.5 kDa, respectively.

Crystal Growth. Five types of sCD4 crystals were grown at two conditions: high salt (≈2 M ammonium sulfate) with 2–3% (vol/vol) PEG 400 and medium salt (≈200 mM ammonium sulfate) with 30–40% PEG 400 (Fig. 2 and Table 1). In both cases, droplets showed transient phase separation before the appearance of crystals. Although the two conditions produced different crystal types, this does not imply that the two conditions are extremely different; variations about the same high salt condition also induced crystal polymorphism. It is tempting to speculate that the composition of salt and PEG in the transient phase at incipient crystallization is essentially identical even though the two overall conditions are considerably different. Nonetheless, the medium salt crystallizations were more sensitive to charge heterogeneity requiring desialated sCD4 for crystal growth, whereas the

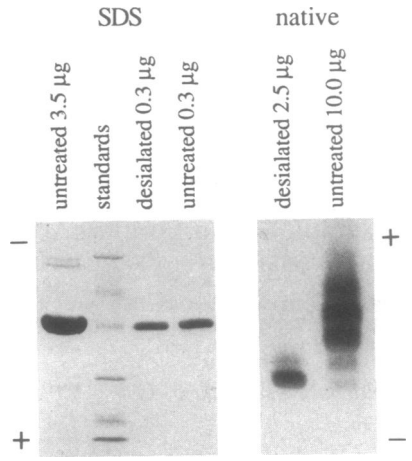

FIG. 1. PAGE of native and desialated sCD4. Gels were electrophoresed on a Pharmacia Phast system and stained with Coomassie R-350. In lanes labeled SDS, 0.1% SDS/PAGE (PhastGel, gradient 10–15%) was used; standards are from Bio-Rad (97.4, 66.2, 42.7, 31.0, 21.5, and 14.4 kDa) with sCD4 migrating at ≈43 kDa. In lanes labeled native, pH 8.8 native PAGE (PhastGel, gradient 8–25%) was used; since sCD4 is positively charged at pH 8.8, the samples were applied to preequilibrated gels and electrophoresed in reverse direction, from anode to cathode. Material contained in various lanes is indicated.

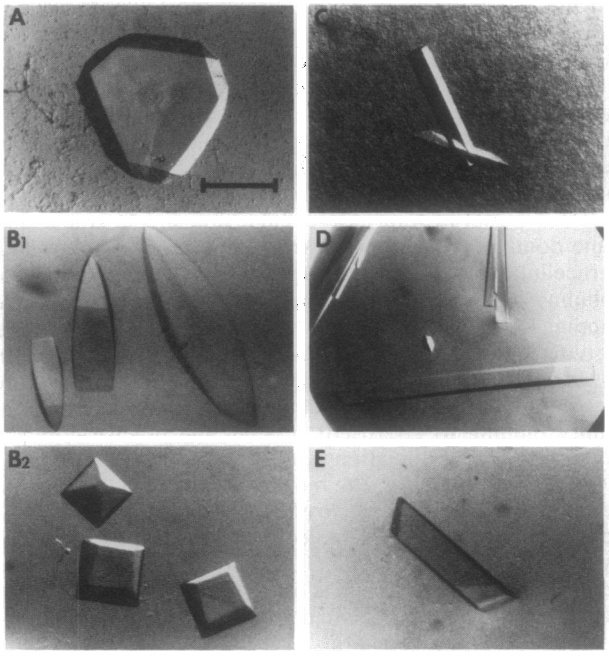

FIG. 2. Crystals of recombinant CD4. (*A*) Trigonal. (B_1) Tetragonal, from citrate. (B_2) Tetragonal, from sulfate. (*C*) Tetragonal, from PEG 400. (*D*) Monoclinic (*P*2). (*E*) Monoclinic (*C*2). (In *A*, bar is 0.35 mm.)

Table 1. Crystallization conditions of sCD4

Crystal type	Initial crystallization droplet*	Equilibrium reservoir and temperature†
A	0.23% PEG 400/183 mM ammonium phosphate/40 mM sodium phosphate/10 mM Tris·HCl/3.1 mM NH_4OH/sCD4 (4.0 mg/ml), pH 8.2	39.0% sat. $(NH_4)_2SO_4$/100 mM Tris·HCl/74 mM NH_4OH, pH 8.7, 20°C
B_1	0.875% PEG 400/425 mM ammonium citrate/25 mM Tris·HCl/25 mM sodium phosphate/sCD4 (2.4 mg/ml), pH 8.5	1.70 M ammonium citrate, pH 8.65, 4°C
B_2	1.0% PEG 400/23.0% sat. $(NH_4)_2SO_4$/50 mM Tris·HCl/10 mM sodium cacodylate/2.5 mM $MnCl_2$/sCD4 (5.0 mg/ml), pH 8.1	55.0% sat. $(NH_4)_2SO_4$/83 mM Tris·HCl/1.7% PEG 400, pH 8.4, 4°C
C	1.4% PEG 400/10.7 mM $(NH_4)_2SO_4$/4.3 mM sodium cacodylate/3.6 mM Tris·HCl/1.2 mM $(NH_4)_3BO_3$/sCD4‡ (2.2 mg/ml), pH 8.0	40.0% PEG 400/100 mM Tris·HCl/49.3 mM NH_4OH, pH 8.8, 20°C
D	2.0% PEG 400/15 mM $(NH_4)_2SO_4$/6.0 mM sodium cacodylate/5.0 mM Tris·HCl/sCD4‡ (3.1 mg/ml), pH 7.5	30.0% PEG 400/100 mM Tris·HCl/29.6 mM NH_4OH, pH 8.7, 4°C
E	1.0% PEG 400/21.0% sat. $(NH_4)_2SO_4$/50 mM Tris·HCl/10 mM sodium cacodylate/2.5 mM $CaCl_2$/sCD4 (5.0 mg/ml), pH 8.1	51.0% sat. $(NH_4)_2SO_4$/83 mM Tris·HCl/1.7% PEG 400, pH 8.4, 20°C

sat., Saturated.
*Composition prior to equilibration with reservoir. Droplet volumes were initially 5–10 μl.
†Equilibration and crystal growth temperature. Crystallizations were set up at room temperature.
‡Asialo sCD4 is required.

high salt crystallizations were not affected by desialation. We do not yet have chemical characterization for the transient phase.

The use of low molecular weight PEG in combination with high salt has been investigated (16) with the finding that the PEG-induced phase separation enhances nucleation by concentrating protein into a PEG-rich phase. In these sCD4 crystallizations, however, PEG 400 may function differently. At high ionic strength, sCD4 shows phase separation in the absence of PEG. Low concentrations of PEG modulate the appearance of this phase separation, increasing both protein solubility and the precipitation point in high salt. Although low molecular weight PEG was an essential component of the sCD4 crystallizations reported here, in its absence we were also able to grow crystals: Triangular plates grew from PEG 20,000 and rectangular parallelepipeds grew from PEG 4000. Unfortunately, these crystals were too small to characterize.

Diffraction Characteristics and Flexibility. The distinguishing feature of the diffraction from these sCD4 crystals is that it drops off sharply at Bragg spacings beyond 6 Å (Table 2). Since the crystals are large (0.6 × 0.6 × 0.2 mm for type A) and have average mosaicity (≈0.2° peak widths for type A), such a drop does not reflect misorientation of the crystallites within the crystal or exceptionally small crystallites. Rather the drop results either from chemical heterogeneity of the unit-cell contents or from conformational heterogeneity between unit cells. Although it is difficult to completely rule out chemical heterogeneity, removal of charge heterogeneity (desialation) does not affect the crystallization of or diffraction from crystal types A, B, or F. Moreover, the desialated sCD4 is essentially homogeneous on isoelectric focusing and in both SDS and native PAGE (Fig. 1). Conformational changes may result, at the extremes, from intrinsic flexibility within the crystallized molecule or from poor lattice contacts that allow for rigid-body mobility. In the present case, it seems unlikely that the poor diffraction is solely a result of bad crystal contacts; the five crystal forms have different lattice contacts, yet the diffraction from all five drops off at approximately the same limiting angle.

It appears, then, that the most plausible explanation for the drop-off in diffraction at 6 Å is conformational mobility or thermal motion in the sCD4 molecule. Thermal motion is also indicated by the large amount of mottled diffuse scattering seen in the diffraction (Fig. 3). Much of the scattering is not associated with Bragg reflections; hence it does not arise from coordinated motions of the crystal lattice but from motion within the unit cell (17, 18).

The observed thermal motion may arise from segmental flexibility of the extracellular domains of CD4. Support for this model comes from proteolytic digestion studies: With V8 protease digestion, a 21-kDa fragment consisting of the first two CD4 domains could be isolated (19); we have characterized a chymotryptic cleavage fragment of sCD4 consisting of residues 178–369 (CD4 domains 3 and 4) (20). Both of these proteolytic cleavage products are stable after purification and retain their native conformations, as judged by gp120 and monoclonal antibody binding (S.-E.R. and K. C. Deen, unpublished observations; refs. 19 and 20). These studies suggest a flexible juncture between CD4 domains 2 and 3 analogous to the hinge region of immunoglobulins.

Table 2. sCD4 crystal parameters

Crystal type	Lattice	Space group	Unit cell parameter a, Å	b, Å	c, Å	β/γ	Volume of unit cell, $Å^3 \times 10^{-6}$	Z_a*	Solvent content, %	Diffraction limit, Å†
A	Trigonal	$P3_121$ ($P3_221$)	126		204	120°	2.80	2 (2.1)	76.4	5.1
B_1	Tetragonal	$P4_122$ ($P4_322$)	123		395		6.00	2 (2.1)	85.3	7.5
B_2	Tetragonal	$P4_122$ ($P4_322$)	124		392		6.03	2‡	85.4	8.0
C	Tetragonal	$P4_122$ ($P4_322$)	125		222		3.47	2 (2.2)	74.6	4.9
D	Monoclinic	$P2$	110	125	98	99.5°	1.33	4 (4.4)	66.9	5.2
E	Monoclinic	$C2$	227	168	141	119.8°	4.65	8 (8.5)	62.1	5.9

Unit cell parameters were determined with an accuracy of 1.4% (see text).
*Number of sCD4 molecules per asymmetric unit. Numbers in parentheses refer to experimental results from amino acid analysis. The experimental numbers contain a systematic overassessment (see text).
†Minimum Bragg spacing observed.
‡Assumed from B_1 crystals, not independently determined.

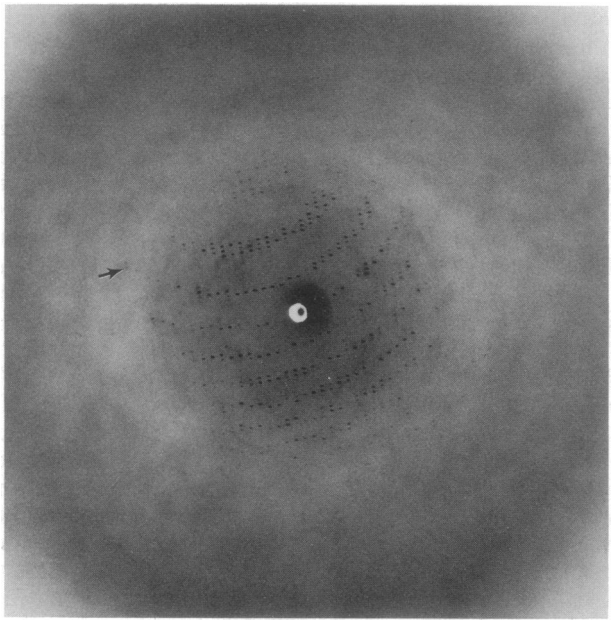

FIG. 3. X-ray diffraction photograph from a sCD4 crystal (type A). Oscillation photograph (2° sector) was taken with 1.22-Å radiation at beam line X12-C, NSLS. The crystal was rotated for 15 oscillations and a total exposure of $\approx 20 \times 10^6$ photons at 20°C with a film–crystal distance of 109 mm. The arrow shows diffraction at 5.5 Å. The ring-like shadow at 6.9 Å is an artifact caused by the Mylar of the helium chamber. The oscillation axis is horizontal and ≈12° from the a^* axis.

Further evidence supporting the proposal that the weak diffraction characteristic of these sCD4 crystals results from segmental flexibility comes from studies on a CD4 fragment that comprises the first two domains (12). This fragment (D_1D_2) does not contain the proposed CD4 "hinge" region. In marked contrast with our results on crystals of the entire extracellular domain, crystals of D_1D_2 diffract to Bragg spacings beyond 2.2 Å (S.-E.R., unpublished observations).

Solvent Content and Z_a Determination. When the diffraction from these sCD4 crystals was first characterized, it was apparent from considerations of unit-cell volume and the size of the sCD4 molecule that, for all the crystal types, the asymmetric unit had an extremely high solvent content, multiple copies of the sCD4 protein, or both.

Typically, characterization of the number of molecules in the asymmetric unit (Z_a) involves measurement of crystal density or symmetry analysis of the Patterson rotation function. However, because of potential difficulties, we used a third method incorporating amino acid analysis to determine Z_a. With this method, the volume of a crystal is measured and then the number of molecules within that crystal volume (which is proportional to Z_a) is determined directly.†† Accurate results were found for all five crystal types, although a systematic (roughly 5%) overassessment of Z_a was found (Table 2). The effect was more pronounced for smaller crystals; nonetheless, with careful attention to crystal drying prior to amino acid analysis, satisfactory results were obtained from crystals as small as 0.16 × 0.06 × 0.06 mm (crystal type C). The measurements reveal two significant features of these sCD4 crystals. (*i*) Some crystal types (e.g., type B) have extremely high solvent contents. (*ii*) All crystals have 2, 4, or 8 copies of the sCD4 molecule in their asymmetric units.

Protein Oligomerization. The universal occurrence of sCD4 molecules in multiples of two per asymmetric unit suggests that sCD4 crystallizes in an associated state. If the associating unit is the same in all crystal types, lattice constraints only permit either a dimer or a tetramer as the fundamental unit. If a dimer, it seems probable that this unit is unsymmetrical; the dyad axes of symmetrical dimers often coincide with crystallographic symmetry axes but none of the crystal types contains a monomer in the asymmetric unit or has a C_4 or D_2 center of symmetry. (Association through only some of the flexibly linked sCD4 domains might lead to this asymmetry.) If a tetramer, it must be a dimer of such possibly nonsymmetric dimers having true molecular dyads necessarily coincident with crystallographic axes in lattices A–C. Interestingly, four of the crystal types (A–D) have crystallographic dyads of approximately the same length (125 ± 2 Å) and the fifth (type E) could accommodate a tetramer as a repeating unit. These results suggest a tetramer with a characteristic dyad length of 125 Å. If the tetrameric association is natural, that is, one that might occur on the surface of a membrane, it would necessarily have cyclic symmetry. Such a tetramer would then be oriented with the four chains in parallel with the four N termini at one end separated from the C termini by 125 Å.

Signal Transduction. CD4 associates intracellularly with a T-cell-specific protein tyrosine kinase ($p56^{lck}$), an association implicated in the regulation of T-cell activation (22). Other receptors, for example the platelet-derived growth factor receptor (23), have been found to oligomerize as a mechanism for signal transduction. If oligomerization is a trigger for signal transduction by CD4, it would necessarily be a rare event in the absence of an appropriate signal (e.g., major histocompatibility complex class II binding); that is, the intrinsic association affinity would be relatively low. Although structural features would reflect a compatibility with this type of association, experiments with CD4 and especially with sCD4, which is not constrained to a membrane surface, would detect this property with difficulty. Gel-filtration experiments show that the recombinant soluble protein does not associate in dilute solution under physiological conditions or at pH 8.8; but in the gel filtration, the concentration of sCD4 did not exceed 0.03 mM. In a crystal, the sCD4 concentration approaches 10 mM. It may be that the extreme sCD4 concentration in the crystal unveils a natural propensity for oligomerization essential to signal transduction. This propensity may be seen only at extreme CD4 concentrations. In the absence of an external signal, dimer formation would be related to the square of the protein concentration and tetramer formation would be related to the fourth power of the protein concentration. Indeed, concentration may be a biologically relevant trigger for CD4; cell adhesion with capping could drive the membrane-bound local concentration of CD4 to extreme levels.

Structural Implications of High Solvent. High solvent content coupled with the crystallization requirement for forming protein–protein lattice contacts places constraints on the shape of the CD4 molecule. Solvent contents of >85% are rare; a survey of the 1025 entries in the crystallization data base (G. L. Gilliland, from Protein Data Bank deposit) shows <2% with solvent contents as high as this. For proteins, high solvent content was found to be strongly indicative of an extended molecular structure, where the length of the folded molecule greatly exceeds the gyration radius of the denatured molecule. This is exemplified by the ≈96% solvent crystals of tropomyosin, a protein with molecular dimensions of 15–20 Å cross-section by 410 Å (24). The survey revealed only one violation of this correlation between high solvent and extended structure; crystal form I of ribulose biphosphate carboxylase has ≈86% solvent and a unit cell composed of 12 molecules (25). As is now known from structure determinations for other crystal forms (26), each molecule is a cylinder with a diameter of ≈110 Å and height 100 Å, com-

††This method is a generalization of one applied to heme-containing crystals (21). Further details will be published elsewhere.

posed of 16 globular subunits (L_8S_8) arranged around a central hole containing a molecular fourfold axis. With the form I crystals, multiple subunits enclose solvent within the molecule; this combined with a loosely packed open lattice results in high overall solvent content. Because of the disparity between the number of subunits needed to generate high solvent (as seen with ribulose biphosphate carboxylase) and the number of subunits in the sCD4 crystals, although enclosed solvent may play a role, it is unlikely to be the sole cause of the high solvent content of the sCD4 crystals. The most likely explanation, then, for the high solvent found in these sCD4 crystals is that the sCD4 molecule has an extended structure.

Ultracentrifugation. The observed sedimentation coefficient was determined to be 2.87 S, yielding a frictional ratio of 1.6. The frictional ratio, f/f_0, results from a component due to shape, f_e/f_0, and a component due to hydration, f/f_e. These are related by the equation, $f/f_0 = (f/f_e)(f_e/f_0)$ (27). The component due to hydration may be computed from the equation $f/f_e = (1 + w/\bar{v}\rho)^{1/3}$, where w is the water content (g of H_2O per g of protein), $\bar{v}$ is the partial specific volume of sCD4, and ρ is the solvent density. Typical hydration values for soluble globular proteins are between 0.1 and 0.6 g of H_2O per g of protein (28). For a hydration range of 0.35–0.60 g of H_2O per g of protein, the component of the frictional ratio due to shape is determined to be 1.4–1.3, which, if one assumes a prolate ellipsoid, corresponds to an axial ratio of 7.2–5.8. Because carbohydrate (which accounts for ≈10% by weight of sCD4, ref. 15) tends to be highly hydrated, the higher hydration estimate and resultant lower axial ratio are probably more realistic.

Molecular Shape. The high solvent content and weak diffraction from these sCD4 crystals suggests an elongated flexible molecule. Ultracentrifugation studies support these results and inferences from the crystals suggest a molecular length of 125 Å. Although all of these results are consistent, it should be stressed that deductions from the crystals are probabilistic and based on two assumptions, that the fundamental unit of crystallization is the same for all crystal types and this unit is one that might occur naturally on the surface of membranes. With these caveats, if each of the sCD4 domains forms a globular unit with dimensions approximating an immunoglobulin domain, then each sCD4 molecule would have dimensions of roughly 25 × 25 × 125 Å.

These dimensions, coupled with the segmental flexibility proposed above, may be instrumental in the function of CD4 as a cellular receptor. They would allow the molecule to extend beyond the cellular glycocalyx, enhance the efficiency of its interactions by increasing binding kinetics, and permit orientational flexibility during recognition events. Also, since the primary interaction of the human immunodeficiency virus with CD4 is at the N-terminal domain, distal from the membrane, such a length may have implications for viral entry to the cell. Interestingly, the intercellular adhesion molecule 1 (ICAM-1, CD54), which binds to the integrin lymphocyte function-associated antigen 1 (LFA-1) and also acts as a receptor for the major group of rhinoviruses, consists of five unpaired immunoglobulin-like domains that form a segmentally hinged rod of dimensions 190 Å by 20–30 Å (29). The extended flexible structure observed for both CD4 and ICAM-1 may be an important criterion governing the functional role of these molecules in cell–cell and cell–virus interaction.‡‡

‡‡CD4 is the focus of structural studies in several laboratories. Subsequent to the preparation of this manuscript, the crystallization of a rat CD4/Fab complex was reported (30).

We thank Mary Ann Gawinowicz Kolks and Andrew Pound for amino acid analyses. Samples of the sCD4 protein were made available through the efforts of the Departments of Bioprocess Sciences and Protein Biochemistry in the Biopharmaceutical Division of SmithKline Beecham Pharmaceuticals (SB). In particular, we thank Dr. Martin Rosenberg at SB for his encouragement and support of this study. Synchrotron facilities used at Brookhaven National Laboratory are supported by the Department of Energy and by the National Institutes of Health. P.D.K. is supported by a National Science Foundation Graduate Fellowship.

1. Maddon, P. J., Littman, D. R., Godfrey, M., Maddon, D. E., Chess, L. & Axel, R. (1985) *Cell* **42,** 93–104.
2. Williams, A. F. & Barclay, A. N. (1988) *Annu. Rev. Immunol.* **6,** 381–405.
3. Gay, D., Maddon, P., Sekaly, R., Talle, M. A., Godfrey, M., Long, E., Goldstein, G., Chess, L., Axel, R., Kappler, J. & Marrack, J. (1987) *Nature (London)* **328,** 626–629.
4. Sleckman, B. P., Peterson, A., Jones, W. K., Foran, J. A., Greenstein, J. L., Seed, B. & Burakoff, S. J. (1987) *Nature (London)* **328,** 351–353.
5. Doyle, C. & Strominger, J. L. (1987) *Nature (London)* **330,** 256–259.
6. Dalgleish, A. G., Beverly, P. C. L., Clapham, P. R., Crawford, D. H., Greaves, M. F. & Weiss, R. A. (1984) *Nature (London)* **312,** 763–766.
7. Klatzman, D., Champagne, E., Chamaret, S., Gruest, J., Guetard, D., Hercend, T., Gluckman, J.-C. & Montagnier, L. (1984) *Nature (London)* **312,** 767–768.
8. McDougal, J. S., Kennedy, M. S., Sligh, J. M., Cort, S. P., Mawle, A. & Nicholson, J. K. A. (1986) *Science* **231,** 382–385.
9. Maddon, P. J., Dalgleish, A. G., McDougal, J. S., Clapham, P. R., Weiss, R. A. & Axel, R. (1986) *Cell* **47,** 333–348.
10. Peterson, A. & Seed, B. (1988) *Cell* **54,** 65–72.
11. Sattentau, Q. J., Arthos, J., Deen, K., Hanna, N., Healey, D., Beverley, P. C. L., Sweet, R. & Truneh, A. (1989) *J. Exp. Med.* **170,** 1319–1334.
12. Arthos, J., Deen, C. K., Chaikin, M. A., Fornwald, J. A., Sattentau, Q. J., Clapham, P. R., Weiss, R. A., McDougal, J. S., Pietropaolo, C., Maddon, P. J., Truneh, A., Axel, R. & Sweet, R. W. (1989) *Cell* **57,** 469–481.
13. Deen, K. C., McDougal, J. S., Inacker, R., Folena-Wasserman, G., Arthos, J., Rosenberg, J., Maddon, P. J., Axel, R. & Sweet, R. (1988) *Nature (London)* **331,** 82–84.
14. MacPherson, A. (1982) *Preparation and Analysis of Protein Crystals* (Wiley, New York), pp. 94–97.
15. Carr, S. A., Hemling, M. E., Folena-Wasserman, G., Sweet, R. W., Anumula, K., Barr, J. R., Huddleston, M. J. & Taylor, P. (1989) *J. Biol. Chem.* **264,** 21286–21295.
16. Ray, W. J., Jr., & Puvathingal, J. M. (1986) *J. Biol. Chem.* **261,** 11544–11549.
17. Doucet, J. & Benoit, J. P. (1987) *Nature (London)* **325,** 643–646.
18. Casper, D. L. D., Clarage, J., Salunke, D. M. & Clarage, M. (1988) *Nature (London)* **332,** 659–662.
19. Ibegbu, C. C., Kennedy, M. S., Maddon, P. J., Deen, K. C., Hicks, D., Sweet, R. W. & McDougal, J. S. (1989) *J. Immunol.* **142,** 2250–2256.
20. Healey, D., Dianda, L., McDougal, J. S., Moore, J. P., Moore, M. J., Estess, P., Kwong, P. D., Buck, D., Beverley, P. C. L. & Sattentau, Q. J. (1990) *J. Exp. Med.*, in press.
21. Hendrickson, W. A., Love, W. E. & Murray, G. C. (1968) *J. Mol. Biol.* **33,** 829–842.
22. Barber, E. K., Dasgupta, J. D., Schossman, S. F., Trevillyan, J. M. & Rudd, C. E. (1989) *Proc. Natl. Acad. Sci. USA* **86,** 3277–3281.
23. Heldin, C.-H., Ernlund, A., Rorsman, C. & Rönnstrand, L. (1989) *J. Biol. Chem.* **264,** 8905–8912.
24. Philips, G. N., Jr., Lattman, E. E., Cummins, P., Lee, K. Y. & Cohen, C. (1979) *Nature (London)* **278,** 413–417.
25. Baker, T. S., Eisenberg, D., Eiserling, F. A. & Weissman, L. (1975) *J. Mol. Biol.* **91,** 391–399.
26. Andersson, I., Knight, S., Schneider, G., Lindqvist, Y., Lundqvist, T., Brändén, C.-I. & Lorimer, G. H. (1989) *Nature (London)* **337,** 229–234.
27. Oncley, J. L. (1941) *Ann. N.Y. Acad. Sci.* **41,** 121–150.
28. Kuntz, I. D. & Kauzman, W. (1974) *Adv. Protein Chem.* **28,** 239–345.
29. Staunton, D. E., Dustin, M. L., Erickson, H. P. & Springer, T. A. (1990) *Cell* **61,** 243–254.
30. Davis, S. J., Brady, R. L., Barclay, A. N., Harlos, K., Dodson, G. G. & Williams, A. F. (1990) *J. Mol. Biol.* **213,** 7–10.